

RESEARCH ARTICLE

Grassland management intensity determines root development, soil structure, and their interrelationship: Results of a regional study of Leptosols in the Swabian Alps

Katrin Kuka¹  | Monika Joschko²

¹Julius-Kühn-Institute (JKI), Institute for Plant and Soil Science, Braunschweig, Germany

²Leibniz Centre for Agricultural Landscape Research (ZALF), Experimental Infrastructure Platform, Müncheberg, Germany

Correspondence

Katrin Kuka, Julius-Kühn-Institute (JKI), Institute for Plant and Soil Science, Bundesallee 58, 38116 Braunschweig, Germany.
Email: katrin.kuka@julius-kuehn.de

Handling Editor: Cory Matthew

Funding information

Deutsche Forschungsgemeinschaft, Grant/Award Number: DFG-Jo228/8-1

Abstract

Background: Soil structure is a key indicator of the functioning of soil processes in grasslands, which is influenced by site conditions and management.

Methods: In this study, we investigated soil structure and its relationship with root growth in 31 Leptosols under different grassland management intensities using X-ray microcomputed tomography. A close relationship between land use intensity, soil structure, and root growth was observed.

Results: Our results show that land use type affects root development and soil structure. Pastures had more developed roots and more structured soils than meadows and mown pastures. However, all pastures were unfertilized, while meadows and mown pastures had both fertilized and unfertilized plots. Although no significant differences were found in the unfertilized plots, sample size was limited. In particular, fertilization negatively affected root growth and soil structure, resulting in significant differences between fertilized and unfertilized grasslands. Mowing frequency also had an effect on soil physics, but to a much lesser extent than fertilization.

Conclusions: Increased land use intensity, characterized by increased fertilization and more frequent mowing, reduces root growth and adversely affects soil structure. Therefore, X-ray microcomputed tomography is a suitable method to investigate the relationship between soil structure and roots in the soil.

KEYWORDS

land use intensity, meadow–mown pasture–pasture, soil structure, root–soil interaction, X-ray microcomputed tomography

INTRODUCTION

Optimal grassland management is imperative for optimizing plant productivity, soil fertility, nutrient and water cycling, soil fauna, and regulation of pests and diseases—integral components of soil health (Doran & Zeiss, 2000). Root development and soil structure are intricately linked to both grassland management and each other. Soil structure can strongly influence plant root growth and vice versa (Pagliai & Nobile, 1993). Soil structure affects the cycling of air, water, and nutrients in the soil and provides habitat for soil biota. Preserving intact soil structure is fundamental for fostering a vital root system (Tracy et al., 2012), while compromised soil structure, like compaction,

can inhibit root growth (Carminati et al., 2009). This can result in reduced plant growth and increased vulnerability to environmental threats.

Root development, in turn, contributes to soil structure dynamics. As roots grow and penetrate the soil, they create channels and spaces that enhance soil aggregation, thereby improving soil structure (Shi et al., 2021). Moreover, plant roots generate organic compounds and enzymes that aid in binding soil particles, forming stable soil aggregates, and facilitating carbon sequestration in the soil (Rillig et al., 2002). The relationship between root development and soil structure is complex and dynamic. Healthy soil structure is important for promoting root growth and their function, while, reciprocally, root development positively

This is an open access article under the terms of the [Creative Commons Attribution-NonCommercial](https://creativecommons.org/licenses/by-nc/4.0/) License, which permits use, distribution and reproduction in any medium, provided the original work is properly cited and is not used for commercial purposes.

© 2024 Julius Kuehn Institute. *Grassland Research* published by John Wiley & Sons Australia, Ltd on behalf of Chinese Grassland Society and Lanzhou University.

influences soil structure over time. Understanding this relationship is important for optimizing soil health and promoting sustainable agricultural practices (Bronick & Lal, 2005; Mayel et al., 2021).

X-ray microcomputed tomography (μ CT) is a powerful imaging technique that can be used to study the interaction between soil and plant roots (Hou et al., 2022). Due to the different X-ray absorption properties of materials with different densities, pores, roots, and soil compartments can be simultaneously visualized and quantified after a single scanning procedure. μ CT scans of undisturbed soil cores or plant pots provide detailed three-dimensional (3D) gray-scale images enabling precise analysis of root architecture, including the distribution of roots, the extent of root branching and the diameter of individual roots, and soil structure parameters, such as porosity and aggregate density (Heijs et al., 1995). This information helps to understand how roots interact with the soil and how soil properties affect root growth and function. In contrast to conventional root washing methods, μ CT provides non-destructive 3D imaging that preserves plant integrity and allows repeated measurements, for example, to study juvenile root development in pots (Blaser et al., 2020). μ CT also has advantages compared to the determination of soil physical parameters using soil cylinders, particularly with regard to the visibility of whether the sample is really undisturbed (Amelung et al., 2023). Disadvantages of μ CT compared to conventional methods can include limited sample size due to the complexity and cost of the measurement and limited sample volume due to the size limitation, which is device-specific, and there is also a trade-off between resolution and sample volume (Zhang et al., 2023).

The potential of simultaneous analysis of soil and roots has been investigated by several authors (Blaser et al., 2020; Perret et al., 2007; Pierret et al., 1999; Schmidt et al., 2012; Tracy et al., 2012). However, studies on the root–soil relationship in soils managed at different intensities are scarce. The root–soil relationship could be an excellent indicator for evaluating management systems on soil structure, which is an important aspect of soil quality (Bronick & Lal, 2005) and soil health since it determines several biological (Chenu & Stotzky, 2002; Hassink et al., 1993) and biogeochemical processes (Juma, 1993; Six et al., 1999; Strong et al., 2004), while roots are of paramount functional importance for plant productivity.

As a first step toward this goal, the relationship between morphological properties of soil structure and root parameters was successfully identified (Kuka et al., 2013). This preliminary study found a positive correlation between soil surface density, a morphological measure of aggregation, and both root volume and root surface density. This was the first time that soil morphology was quantitatively related to root biomass in field soils. Therefore, this method is a good tool to test the effect of soil management on soil quality and soil health (effect on soil structure and effect on root development simultaneously). Results from a preliminary study with a limited data set of three plots (Kuka et al., 2013) further suggested that increasing land use intensity in grassland decreased soil surface density and root biomass. The land use gradient in this previous study

ranged from an unfertilized, extensively grazed plot to a fertilized, mowed pasture. The aim of this study was therefore to apply the above approach to a larger data set.

The relationship between soil structure and root growth in differently managed grassland soils was investigated within the Biodiversity Exploratories Program in the Swabian Alps (Fischer et al., 2010). By focusing on one soil type, Leptosol, we aimed to minimize variation in soil properties that could confound management effects.

By applying μ CT to undisturbed soil cores from grasslands to simultaneously quantify soil structure and root morphology, we tested the following hypotheses: (1) Root development is closely related to soil structure in differently managed grassland sites. (2) Soil parameters are influenced by land use type (pasture, meadow, and mown pasture). (3) Increased land use intensity, characterized by increased fertilization and mowing frequency, reduces root growth and negatively affects soil structure.

MATERIALS AND METHODS

Study area

This study was conducted in the Biodiversity Exploratory “Swabian Alps” (AEG region) in southwestern Germany (Fischer et al., 2010; <http://www.biodiversity-exploratories.de>). The bedrock in the Swabian Alps consists of Jurassic limestone, which explains the relatively high pH between 5 and 7 of the mostly shallow soils. The predominant soil type in the region is the Leptosol. The mean annual temperature is between 6°C and 7°C, and the mean annual precipitation is between 700 and 1000 mm. Out of a total of 50 experimental plots, the 31 grassland (AEG) plots on the predominant Leptosol soil type were selected to ensure comparability and, in particular, to study the management effect on soil structure and root development using μ CT. All experimental plots are 50 m \times 50 m in size and are normally cultivated by farmers in the same way as the surrounding grassland. Grassland management types ranged from extensively to intensively managed pastures, meadows, and mown pastures (Gilhaus et al., 2017). To compare different plots with respect to different grassland uses and their land use intensities, Blüthgen et al. (2012) developed the Land Use Intensity Index (LUI index), which can be calculated annually based on annual nitrogen fertilization, mowing frequency and livestock density standardized relative to its mean value (MV) within the AEG model region using Equation (1):

$$\text{LUI}_{(2006-2011)} = \frac{\text{Fe}}{\text{Fe}_{\text{AEG}}} + \frac{\text{M}}{\text{M}_{\text{AEG}}} + \frac{\text{G}}{\text{G}_{\text{AEG}}}, \quad (1)$$

where Fe is the fertilization level ($\text{kg N ha}^{-1} \text{ year}^{-1}$), M is the mowing frequency per year and G is the grazing intensity, reflected by the density of livestock (livestock units [LU] days of grazing $\text{ha}^{-1} \text{ year}^{-1}$) on each site for a given year and Fe_{AEG} , M_{AEG} , and G_{AEG} their respective mean within the AEG region for that year (i.e., the mean

across all 50 experimental plots in the AEG region). Due to the standardization by ratios, LUI is dimensionless. To determine the land use intensity over a longer period of time before sampling, the LUI index for this study was calculated annually from 2006, the start year of the biodiversity exploratories, to 2011, the year of sampling, to calculate the mean LUI (2006–2011) as well as the increase or decrease of the LUI (LUI slope, LUI_s) and the starting LUI level (LUI intercept, LUI_i). To calculate the linear regression coefficients LUI_i and LUI_s in the linear function Equation (2), the calendar years 2006–2011 were normalized to the period from 0 to 11 years and adjusted with a linear regression model

$$LUI = LUI_i + LUI_s \times \text{year}. \quad (2)$$

Table 1 shows the management parameters and basic soil data and their variation according to grassland use types. Detailed information about management data and site characteristics and all used data (IDs 31514, 14686, 14447, 14446, 16566, 16586) for analysis in this study can be found under <https://www.bexis.uni-jena.de/>.

Soil sampling

Soil sampling was conducted in May 2011, extracting one to three undisturbed soil samples (12 cm in height and diameter) from the topsoil within an assigned 1 m² square of the experimental plots. The accessibility of the experimental plots and the stone content of the soil determined the amount of samples, which were collected using an automated sampling device (Kuka et al., 2013). To ensure

high-resolution μ CT analysis in the laboratory, an adequate sample size is crucial. Therefore, smaller undisturbed soil cores (1–3) of 3 cm height and diameter were collected from the larger soil cores using a second sampling device (Kuka et al., 2013). The different number of samples taken from the field and the different number of smaller sample cores result in a different number of sample replicates (n).

X-ray μ CT

All smaller soil cores were scanned with a resolution of 40 μ m using the 225 kV μ CT scanner at BAM (Bundesanstalt für Materialforschung und -prüfung in Berlin, Germany). This resolution allowed the quantification of roots and solid patterns with individual object sizes >70 μ m (Kuka et al., 2013). The analyses were performed with scanner settings of 210 kV and 12 W emission power in the microfocal range of the tube for a detection time of 1 h. The scanner design was described by Illerhaus et al. (2002).

Quantification of soil structure and root system parameters for all undisturbed soil samples with a sample size of 30 mm in diameter and height was performed using VG StudioMax[®] version 2.1. The analysis method is a combination of histogram analysis (gray values between 0 and 250) and spatial transformation to distinguish between solid, pore and root phases (Kuka et al., 2013). The routine consists of seven steps:

- (1) Remove the acrylic cylinder to obtain only the soil information in the histogram.
- (2) Segmentation of solid part voxels from the histogram (gray values > 81).

TABLE 1 Characterization of grassland land use types in terms of management (LUI, Land Use Intensity Index; G, grazing intensity; M, mowing frequency; Fe, fertilization level) and basic soil data (clay, silt, sand content, PD, pH, C_{tot} , N_{tot} , and CN) on the basis of the BEXIS database (<https://www.bexis.uni-jena.de/>).

Parameter	Meadow				Mown pasture				Pasture			
	MV	Min	Max	SD	MV	Min	Max	SD	MV	Min	Max	SD
LUI	1.9	0.9	2.8	0.5	1.8	1.0	3.5	0.7	0.8	0.6	1.3	0.3
LUI_i	2.0	0.9	2.9	0.6	1.7	0.6	3.4	0.9	0.8	0.5	1.3	0.4
LUI_s	0.0	−0.2	0.1	0.1	0.0	−0.2	0.2	0.1	0.0	0.0	0.1	0.0
G (LU d ha ^{−1} year ^{−1})	0	0	0	0	239	21	1034	284	90	35	198	66
M	2.3	1.0	3.0	0.6	0.9	0.2	2.0	0.5	0.0	0.0	0.0	0.0
Fe (kg N ha ^{−1} year ^{−1})	90.9	0.0	243.4	66.4	37.8	0.0	135.2	42.0	0.0	0.0	0.0	0.0
Clay (%)	59.9	43.6	67.2	7.4	56.6	36.5	70.8	10.1	52.0	38.5	59.9	8.3
Silt (%)	36.6	29.8	51.2	6.4	39.3	27.0	55.4	8.3	41.4	38.5	46.6	2.7
Sand (%)	3.5	1.7	7.7	1.8	4.1	0.8	11.7	3.2	6.6	1.4	18.8	6.9
PD (g cm ^{−3})	2.4	2.3	2.4	0.0	2.4	2.3	2.5	0.0	2.4	2.3	2.5	0.1
pH	6.4	5.5	6.9	0.5	6.1	5.1	6.6	0.4	6.3	5.3	7.1	0.6
C_{tot} (g kg ^{−1})	75.2	61.8	99.3	11.6	72.5	46.5	95.3	17.0	73.6	43.8	104.7	23.4
N_{tot} (g kg ^{−1})	7.4	6.0	9.6	1.2	7.1	4.9	9.2	1.5	5.8	4.1	8.1	1.5
CN	10.0	9.5	10.4	0.3	10.2	9.2	11.2	0.6	11.2	10.6	11.9	0.5

Note: The numbers of plots for meadow, mown pasture, and pasture are 12, 12, and 7, respectively.

Abbreviations: CN, carbon:nitrogen ratio; C_{tot} , total carbon; i, intercept; LU, livestock unit; max, maximum; min, minimum; MV, mean value; N_{tot} , total nitrogen; PD, particle density; s, slope; SD, standard deviation.

- (3) Spatial transformation (dilatation of the solid space +1 voxel and inversion) to obtain the spatial information of the pore/root space -1 voxel without histogram information, followed by liquidation of the root/solid mixed voxels.
- (4) Copying the spatial information of the whole sample to obtain the histogram information of the pore/root space (size -1 voxel).
- (5) Root selection (size -1 voxel).
- (6) Dilatation of the root space +1 voxel to obtain the correct root space size.
- (7) Estimate the pore space as the difference between the total volume and the combined volume of solids and roots.

The segmentation method is described in detail in Kuka et al. (2013). The method determined the following parameters: pore volume (PV, %), solid volume (SV, %), root volume (RV, %), solid surface (SSurf, $\text{m}^2 \text{m}^{-3}$ soil), root surface (RSurf, $\text{m}^2 \text{m}^{-3}$ soil) and SSurf (m^2)/volume (m^3) ratio equal surface density (SDen, m^{-1}).

Statistics

All statistical analyses were conducted using the open-source software R version 4.1.3 (R Core Team, 2021). We investigated the effects of land use types (pasture, meadow, or mown pasture) and its intensity, such as fertilization (unfertilized and fertilized plots) and mowing frequency (0–3 cuts per year), on soil and root parameters determined by μCT by plotting the data as boxplots using ggplot2 (Wickham et al., 2016) and testing for significant differences using a post hoc test using the emmeans function (Russell, 2023). The function ggplot2 (method lm) was used to represent the relationship between the soil and root parameters determined by μCT separately for the utilization types and unfertilized and fertilized plots by means of a regression. Linear models (LMs) were compared to analyze which of the grassland management practices Fe, M, and/or G influence the soil and root parameters determined by μCT and how LUI, LUI_i, and LUI_s as integrating parameters of Fe, M, and G influence them. First, the MVs of Fe, G, M, and LUI between 2006 (start of biodiversity exploratories) and 2011 (time of sampling) were calculated for each plot to take into account the long-term effect of management measures. For the LUI_i and the LUI_s, there is only one value for each plot. Then, MVs of Fe, G, and M as predictor variables were square root-transformed for use in the LM models. All dependent variables PV, SV, RV, SSurf, Rsurf, and SDen were log-transformed. The LM models were generated separately for Fe, G, and M, as well as for LUI, LUI_i, and LUI_s and fitted with main effects and two-way interactions using the function glmulti (Calcagno, 2013). All candidate models were ranked according to the corrected Akaike information criterion (AICc), where lower AICc values indicate a better trade-off between model fit and complexity (Akaike, 1973). Additionally, we used the difference in AICc (dAICc), which was calculated by subtracting the AICc of the model with the lowest AICc from the AICc of each model. Smaller differences (closer to zero) indicate a better-performing model. However, models

with a dAICc of <2 are often considered comparatively good. The best models for all dependent variables were interpreted using the effects function (Fox, 2003) and the ggfortify function (Tang et al., 2016). Because LUI is an integrating parameter for Fe, M, and G, we also interpreted these LM models.

RESULTS

Qualitative μCT results

Figure 1 shows a representative example from each plot, with a two-dimensional μCT image of the soil next to the corresponding 3D μCT image of the roots. Figure S1 shows two additional replicates for each of the specified land use types, highlighting visual similarities between replicates from an unfertilized pasture, an unfertilized meadow, a fertilized meadow, an unfertilized mown pasture and a fertilized mown pasture. Initial observations suggest a potential relationship between soil structure and rooting pattern. Notably, plots AEG02, 04, 07, 08, 09, 10, 22, 24, 27, 28, 30, and 32, characterized by highly structured soils, show a dense root system. In contrast, compacted soils in plots AEG03, 05, 06, 11, 15, and 34 display a sparse root system. In some samples, such as AEG04, 05, 14, 31, and 33, the presence of root nodules is observed.

Quantitative μCT results

The μCT parameters, including SV, RV, PV, SSurf, RSurf, and SDen, were determined for all the plots (Table 2). Notably, plot AEG25, an unfertilized pasture with a relatively low LUI, has the lowest percentage of SV and the highest percentage of RV, as well as the highest SSurf, RSurf, and SDen. Conversely, plot AEG15, a fertilized meadow with a relatively high LUI, has the highest percentage of SV, coupled with the lowest RV and RSurf. Plot AEG05, a fertilized mown pasture with a medium LUI, records the lowest SSurf and SDen. Plot AEG11, a fertilized meadow with relatively high LUI, has the lowest PV, while plot AEG27, an unfertilized pasture with a moderate LUI, has the highest PV.

Impact of grassland management on soil and root parameters

In some cases, significantly different μCT parameters were determined for different land use types (Figure 2). The post hoc tests revealed that pastures have a significantly higher mean SSurf of $3844 \text{ m}^2 \text{m}^{-3}$ soil (p : 0.028, residual standard error: 557.2 with 28 degrees of freedom, F : 4.10, R^2 : 0.23), a significantly higher mean SDen of $8.25 \times 10^4 \text{ m}^{-1}$ (p : 0.032, residual standard error: 23.1 with 28 degrees of freedom, F : 3.92, R^2 : 0.22), a significantly higher mean RV of 14% (p : 0.020, residual standard error: 3.9 with 28 degrees of freedom, F : 4.49, R^2 : 0.24) and a significantly higher mean RSurf of $1694 \text{ m}^2 \text{m}^{-3}$ soil (p : 0.029, residual standard error: 503.8 with 28 degrees

of freedom, F : 4.03, R^2 : 0.22). The model assumptions for the analysis of variance (ANOVA) (homogeneity of variance and approximately normal distribution of the residuals) were checked visually in each case. This implies

that pasture has a significant influence on root development and soil structure. However, when focusing on unfertilized plots from Table 1, no significant differences are observed between meadows, mown pastures and

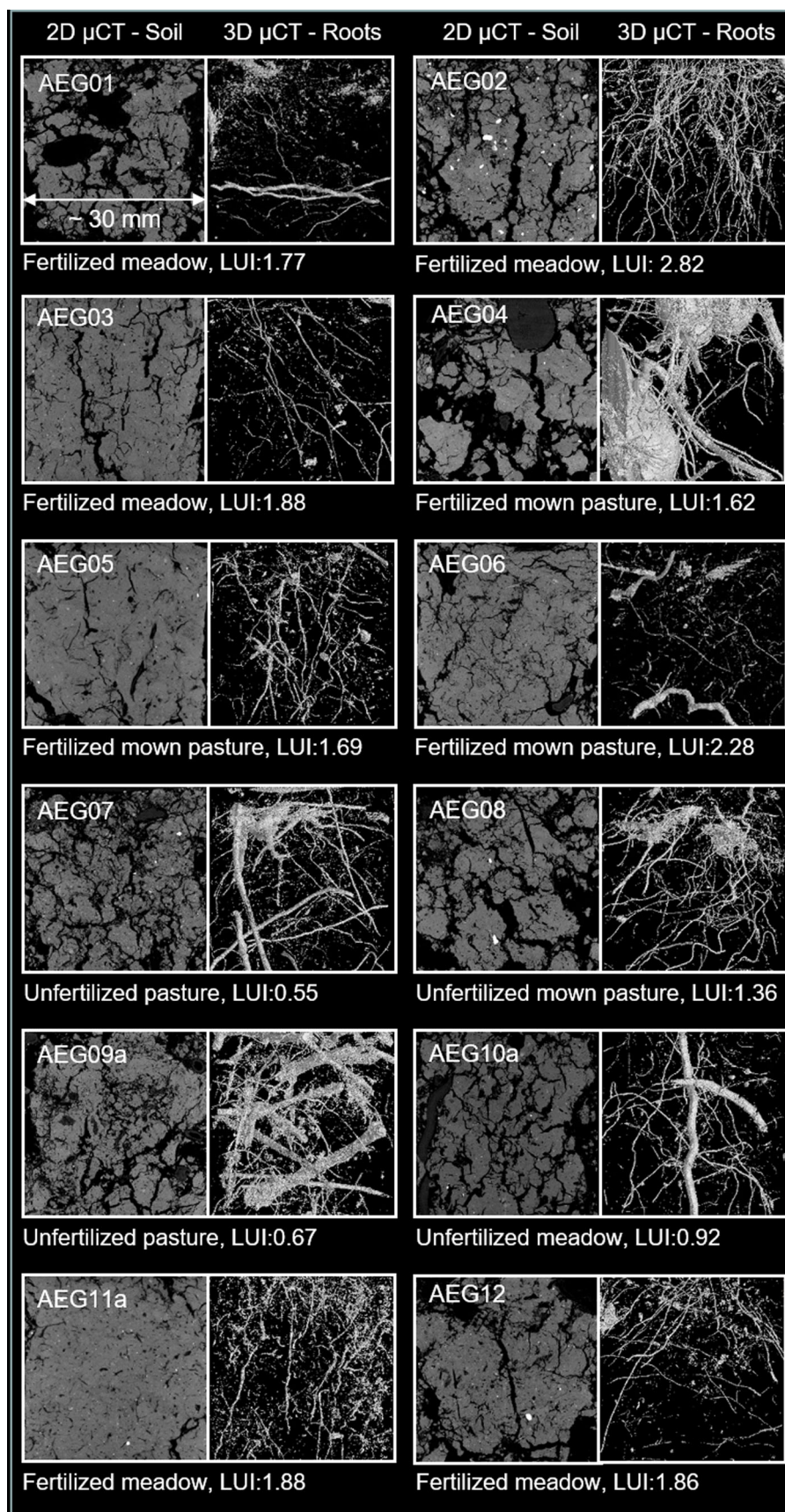


FIGURE 1 Two-dimensional microcomputed tomography (μ CT) soil and three-dimensional μ CT root images of all AEG Leptosol plots including information on fertilization, land use, and land use intensity.

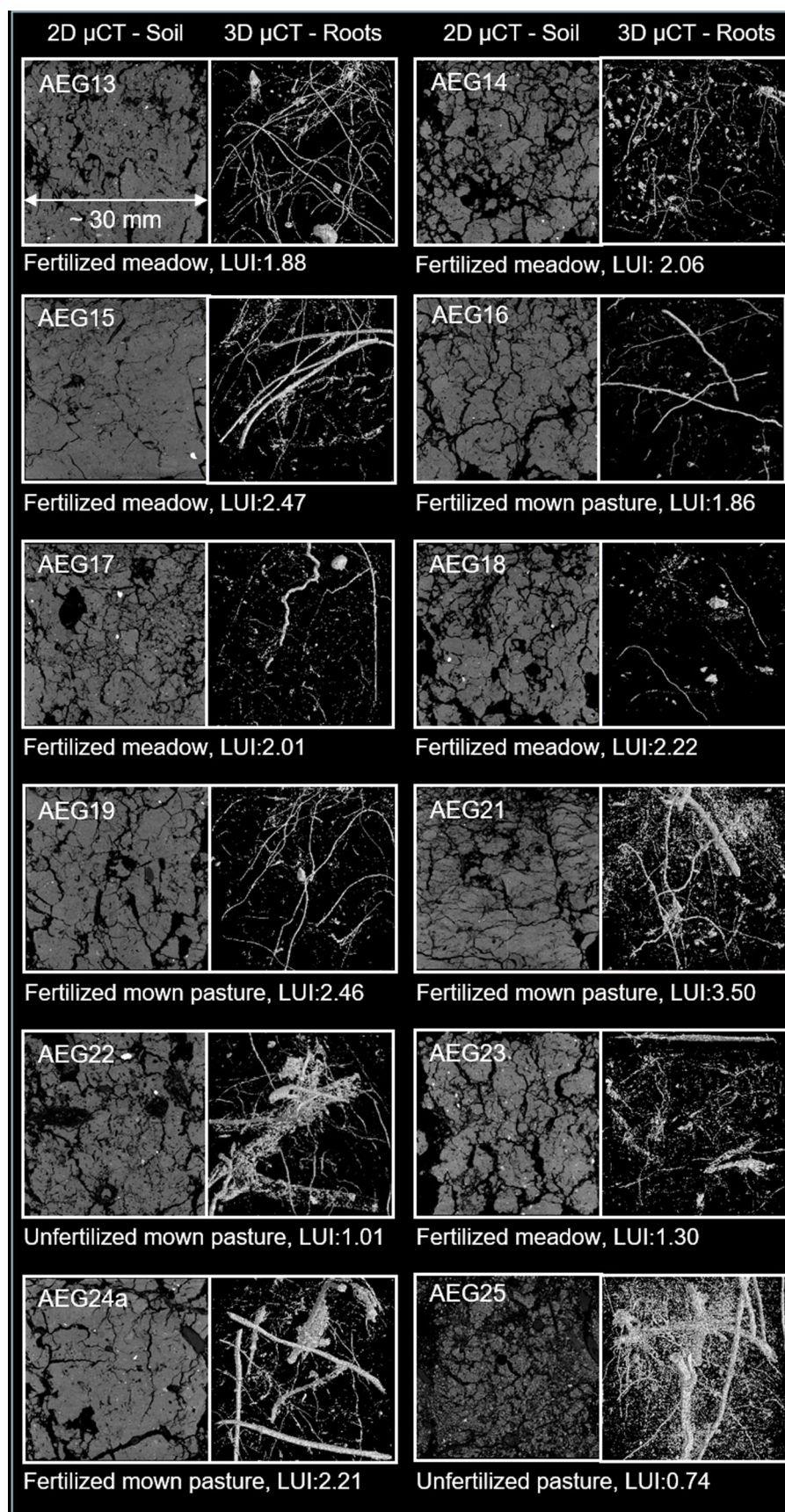


FIGURE 1 (Continued)

pastures. The limited number of samples, with only one unfertilized meadow, may contribute to this lack of significance. Therefore, we present results for all plots together, regardless of their fertilization status.

In comparing the measured μ CT parameters for fertilized and unfertilized plots (Figure 3), all parameters, except PV, are significantly different. The post hoc tests revealed that unfertilized plots have a significantly lower

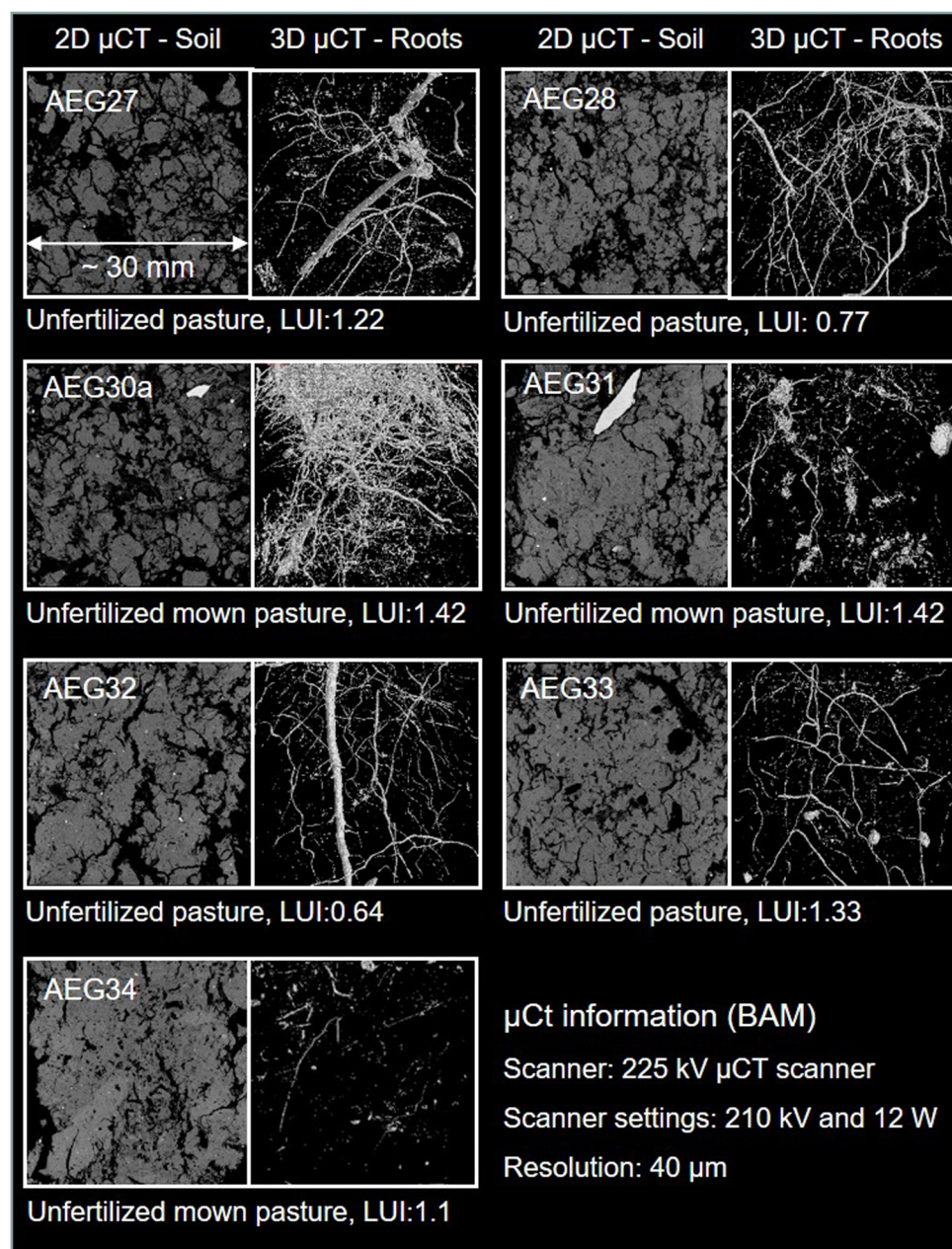


FIGURE 1 (Continued)

mean SV of 52.8% (p : 0.012, residual standard error: 9.6 with 29 degrees of freedom, F : 7.23, R^2 : 0.20), a significantly higher mean SSurf of $3696 \text{ m}^2 \text{ m}^{-3}$ soil (p : 0.002, residual standard error: 529.4 with 29 degrees of freedom, F : 11.1, R^2 : 0.28), a significantly higher mean SDen of $7.48 \times 10^4 \text{ m}^{-1}$ (p : 0.008, residual standard error: 22.7 with 29 degrees of freedom, F : 8.26, R^2 : 0.22), a significantly higher mean RV of 12.66% (p : 0.006, residual standard error: 3.9 with 29 degrees of freedom, F : 8.99, R^2 : 0.24) and a significantly higher mean RSurf of $1526 \text{ m}^2 \text{ m}^{-3}$ soil (p : 0.006, residual standard error: 492.4 with 29 degrees of freedom, F : 8.76, R^2 : 0.23). The model assumptions for the ANOVA (homogeneity of variance and approximately normal distribution of the residuals) were checked visually in each case. This analysis indicates a significant increase in root growth in the unfertilized plots, which is associated with a higher degree of soil structural organization.

Mowing frequency has an effect on soil and root parameters and there is a tendency that more cuts per year are correlated with a lower soil structure and lower root development (Figure 4). However, the post hoc test showed that only the SV was significantly higher (p : 0.07595, residual standard error: 9.857 with 27 degrees of freedom, F : 2.559, R^2 : 0.2214), with a mean of 68.2% at a mowing frequency of three times per year compared to less frequent mowing. The model assumptions for the ANOVA (homogeneity of variance and approximately normal distribution of the residuals) were checked visually.

Relationship between soil structure and root development

The relationships between various soil structure and root parameters show significant variations across

TABLE 2 Results of μ CT analysis for SV, RV, PV, SSurf, RSurf, and SDen (surface density).

Plot	SV (%)	SD SV (%)	RV (%)	SD RV (%)	PV (%)	SD PV (%)	SSurf ($\text{m}^2 \text{m}^{-3}$ soil)	SD SSurf ($\text{m}^2 \text{m}^{-3}$ soil)	RSurf ($\text{m}^2 \text{m}^{-3}$ soil)	SD RSurf ($\text{m}^2 \text{m}^{-3}$ soil)	SDen (10^3m^{-1})	SD SDen (10^3m^{-1})	n
AEG01	42.3	7.2	11.0	4.8	46.7	3.2	3341	173	1750	789	81	19	3
AEG02	58.5	7.4	9.4	1.7	32.1	8.0	2824	358	1216	209	49	8	7
AEG03	68.1	7.6	7.6	2.0	24.3	8.9	2759	267	971	245	41	3	6
AEG04	66.8	16.4	10.3	6.2	22.9	10.6	2421	691	921	114	37	8	4
AEG05	70.5	11.2	6.0	1.5	23.5	12.5	2096	330	590	84	30	7	5
AEG06	63.4	5.2	9.8	3.5	26.8	7.4	2640	362	928	207	42	6	7
AEG07	49.0	3.0	16.4	1.2	34.6	4.1	4344	290	1972	58	89	10	3
AEG08	49.1	4.6	11.5	3.7	39.4	6.0	3084	536	1378	219	63	8	8
AEG09	56.1	6.1	15.6	4.2	28.3	6.0	3335	705	1539	330	61	18	6
AEG10	52.1	2.9	10.5	0.9	37.3	2.2	3975	260	1442	180	77	10	3
AEG11	77.4	3.9	11.5	3.1	11.1	1.9	2978	735	777	218	39	11	6
AEG12	55.6	3.8	7.2	0.8	37.2	4.6	3144	282	1037	90	57	3	3
AEG13	56.7	8.0	9.1	1.4	34.2	6.8	3311	323	1221	263	59	3	3
AEG14	54.9	1.9	6.0	1.0	39.1	0.9	3159	402	836	214	58	9	2
AEG15	82.7	0.8	4.6	1.1	12.7	1.8	2910	177	385	34	35	2	3
AEG16	60.2	8.3	6.9	2.6	32.9	6.1	3275	114	884	334	55	9	3
AEG17	59.9	7.1	9.3	0.5	30.8	7.1	3935	212	1018	56	66	6	3
AEG18	62.6	3.9	5.4	0.6	32.0	4.4	3292	90	749	60	53	4	3
AEG19	58.4	9.7	8.3	2.4	33.3	8.1	3203	83	1057	295	56	9	3
AEG21	55.7	12.2	11.8	2.1	32.5	14.3	3469	790	1267	110	62	1	2
AEG22	63.0	1.7	10.0	0.2	27.0	1.5	3655	154	1140	73	58	1	2
AEG23	53.4		11.0		35.6		3168		1557		59		1
AEG24	73.4	4.6	6.8	0.8	19.8	3.8	3049	351	761	109	41	2	2
AEG25	32.8	1.8	27.1	6.4	40.1	7.6	5568	459	3388	329	170	8	3
AEG27	41.4	3.4	11.7	3.1	46.9	6.5	3813	486	1625	316	92	6	3
AEG28	56.3	1.7	9.3	2.0	34.5	2.2	3328	376	1234	303	59	8	3
AEG30	41.2	2.6	15.4	2.6	43.3	3.6	3564	225	1938	233	86	1	3
AEG31	59.8	5.2	13.7	5.6	26.5	0.4	3492	743	1333	202	58	7	2
AEG32	60.6	2.7	7.8	1.0	31.6	1.9	3331	117	948	87	55	1	3
AEG33	62.0	7.5	10.1	4.3	27.9	9.5	3189	195	1153	296	52	4	3
AEG34	63.0	2.1	5.4	0.7	31.5	1.8	3371	372	752	84	54	8	3

Abbreviations: n, number of replications; PV, pore volume; RSurf, root surface; RV, root volume; SD, standard deviation; SDen, surface density; SSurf, solid surface; SV, solid volume; μ CT, microcomputed tomography.

different land use types (Figure 5). Although SV increases with decreasing PV in all cases, the correlation is significantly closer for meadows and mown pastures compared to pastures. The relationship between RV and SV also differs significantly among land use types. Meadows show no correlation, while on mown pastures and pastures, RV decreases with increasing SV or vice versa. In pastures, the relationship between root development and soil structure is more pronounced. Increased RV and RSurf lead to a significant increase in SDen.

The relationship between root and soil parameters shows differences between fertilized and unfertilized plots (Figure 6). In fertilized plots, there is a strong negative correlation between PV and SV, while there is no discernible relationship between RV and SV or SDen. Although there is also a negative correlation between PV and SV in unfertilized plots, it is lower than that in fertilized plots. Conversely, a negative correlation between RV and SV and a positive correlation between RV and SDen are observed in unfertilized plots, along with a very close positive correlation between RSurf and SDen.

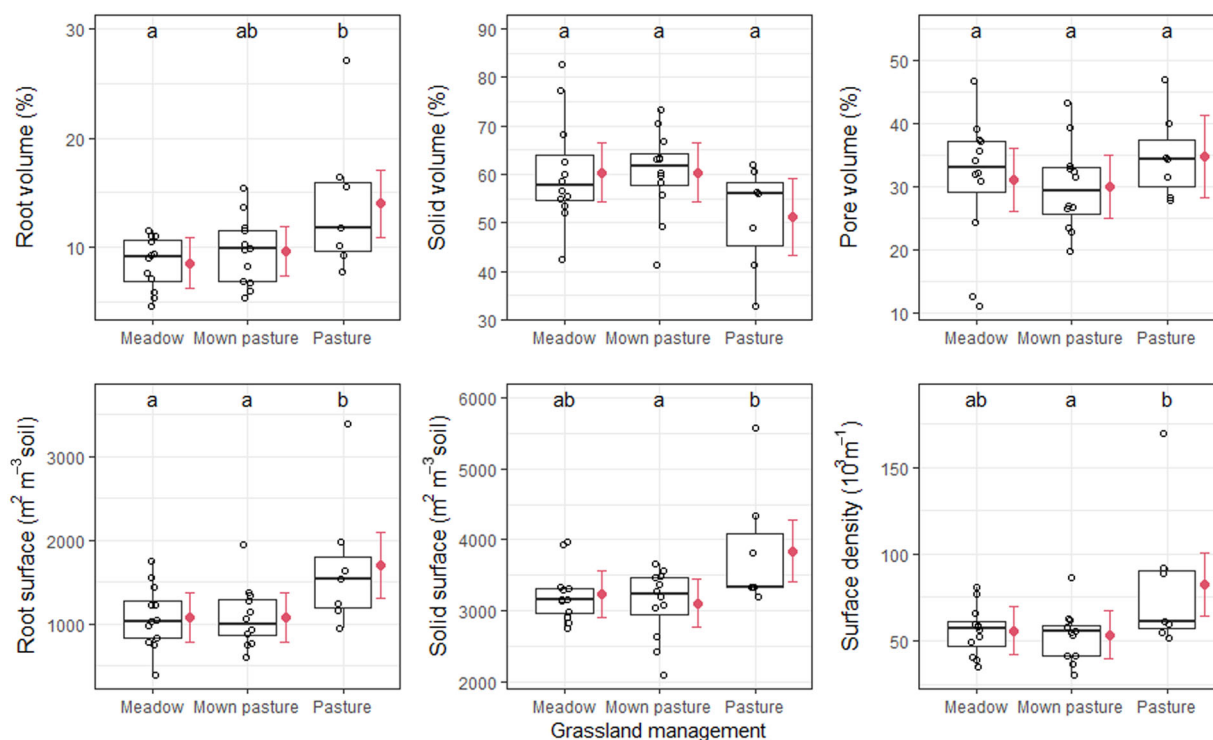


FIGURE 2 Boxplots of all the measured microcomputed tomography parameters, subdivided for different types of grassland management. Grassland use types that do not share a letter are significantly different ($p < 0.05$).

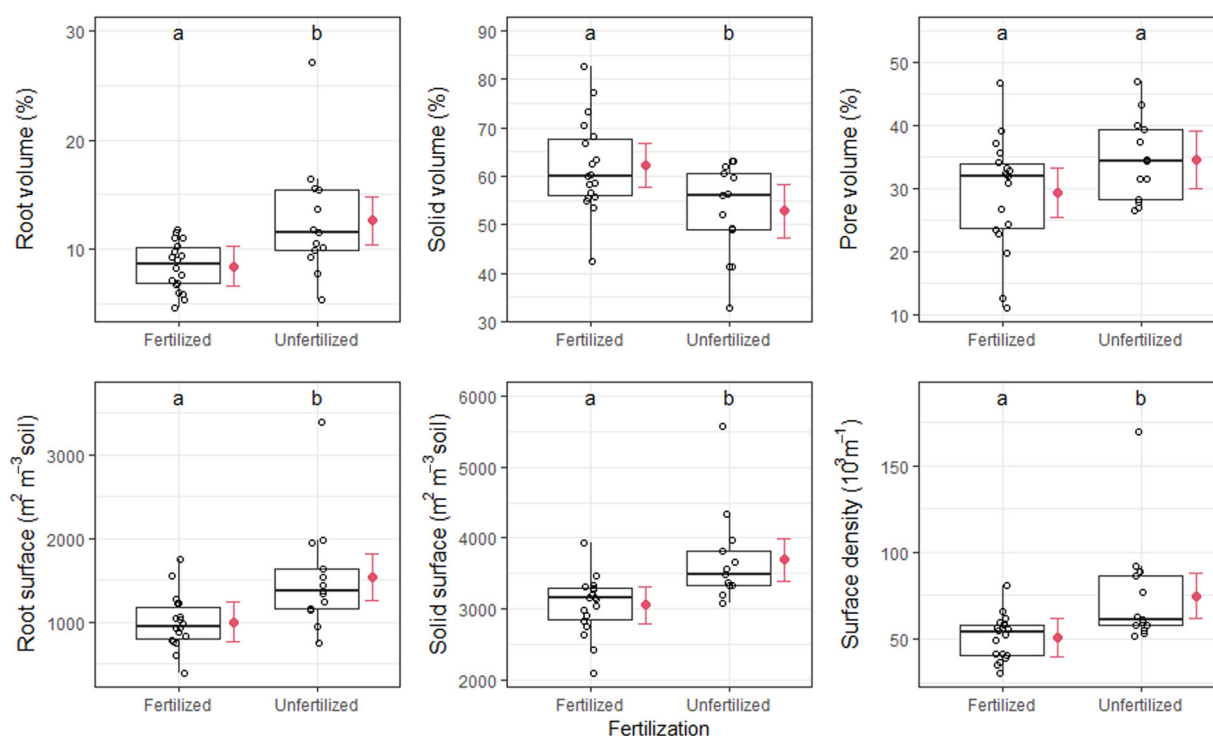


FIGURE 3 Boxplots of measured microcomputed tomography parameters, divided into unfertilized and fertilized plots, which are significantly different if the letters differ ($p < 0.05$).

Impact of land use intensity on root development and soil structure

To test which grassland management measures influence the soil and root parameters determined by μCT and to what extent, different LM models with the parameters G,

Fe, M, or LUI, LUI_i , and LUI_s were compared as candidate models. Except for PV, Fe was the most important predictor variable for all μCT parameters (Table 3). Fe alone explains 18% to 27% (see R^2 in Table 4) of the variance of the dependent variables. Fe has a particular effect on root growth. As Fe increases, RV

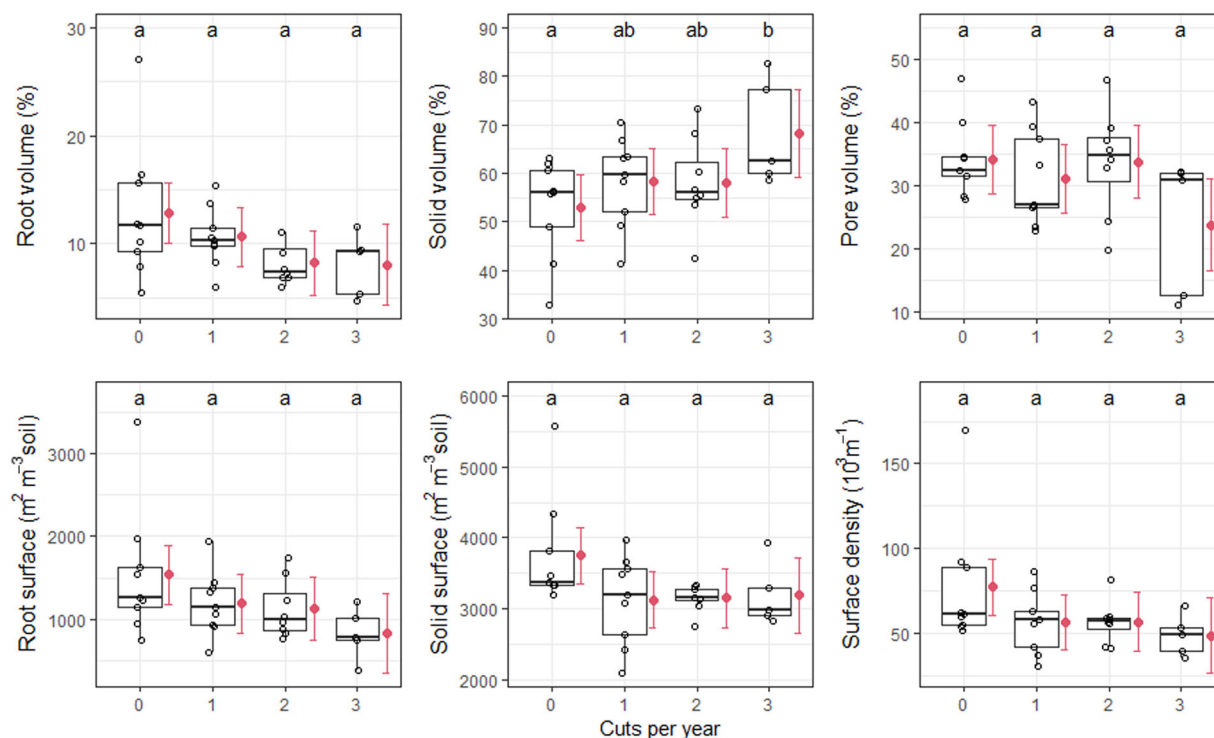


FIGURE 4 Boxplots of all measured microcomputed tomography parameters according to mowing frequency (0 = all pastures without cuts), which are significantly different if the letters differ ($p < 0.05$).

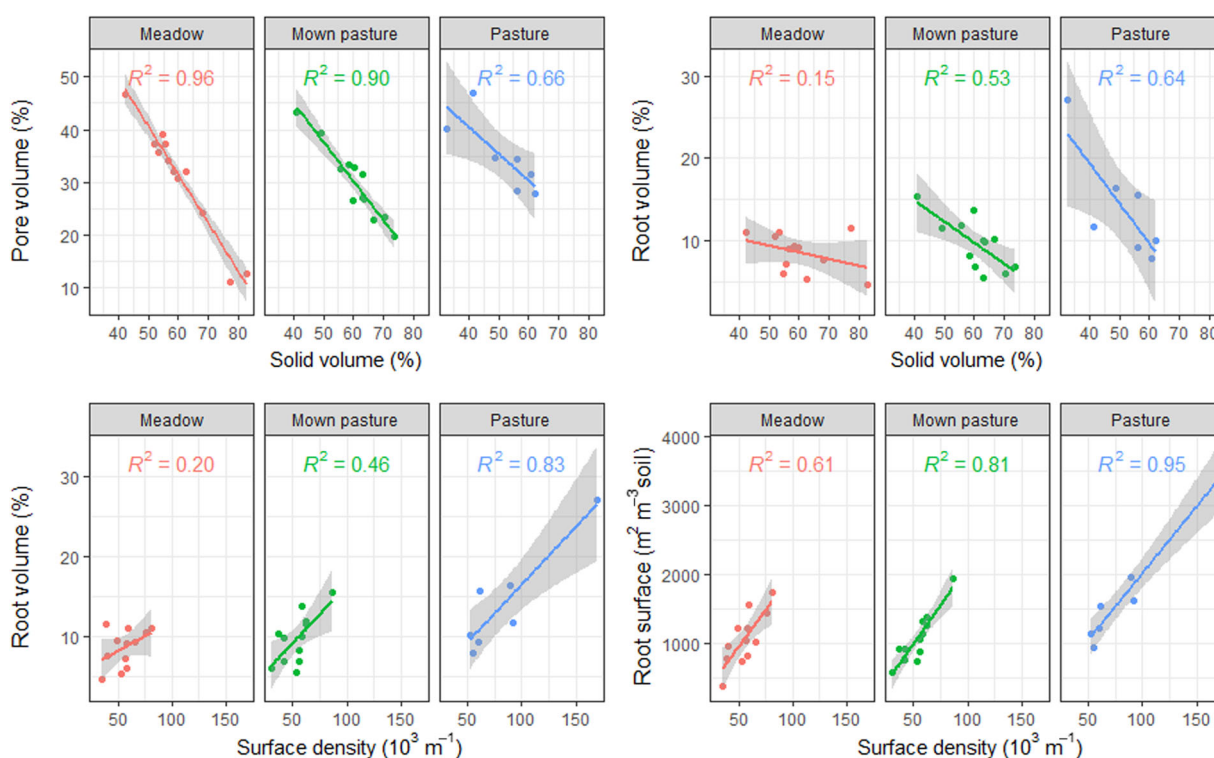


FIGURE 5 Relationship between soil structure and root development depending on grassland use as regression lines with 95% confidence intervals.

and RSurf decrease significantly ($p < 0.01$). Looking at the results of the RV-LM model (Figure 7 and Table 4), the RV of the unfertilized plots is about 12%, with an Fe of $50 \text{ kg N ha}^{-1} \text{ year}^{-1}$ on average only 9% (RV decrease compared to unfertilized plots by 24%) and with an Fe of $200 \text{ kg N ha}^{-1} \text{ year}^{-1}$ on average only 7% (RV decrease

compared to unfertilized plots by 43%). The RSurf LM model also predicts similar percentage decreases, which are 27% for an Fe of $50 \text{ kg N ha}^{-1} \text{ year}^{-1}$ and 46% for an Fe of $200 \text{ kg N ha}^{-1} \text{ year}^{-1}$ of the average RSurf of approximately $1400 \text{ m}^2 \text{m}^{-3} \text{soil}$ for unfertilized plots. Fe also has a negative effect on soil structure, with a decrease

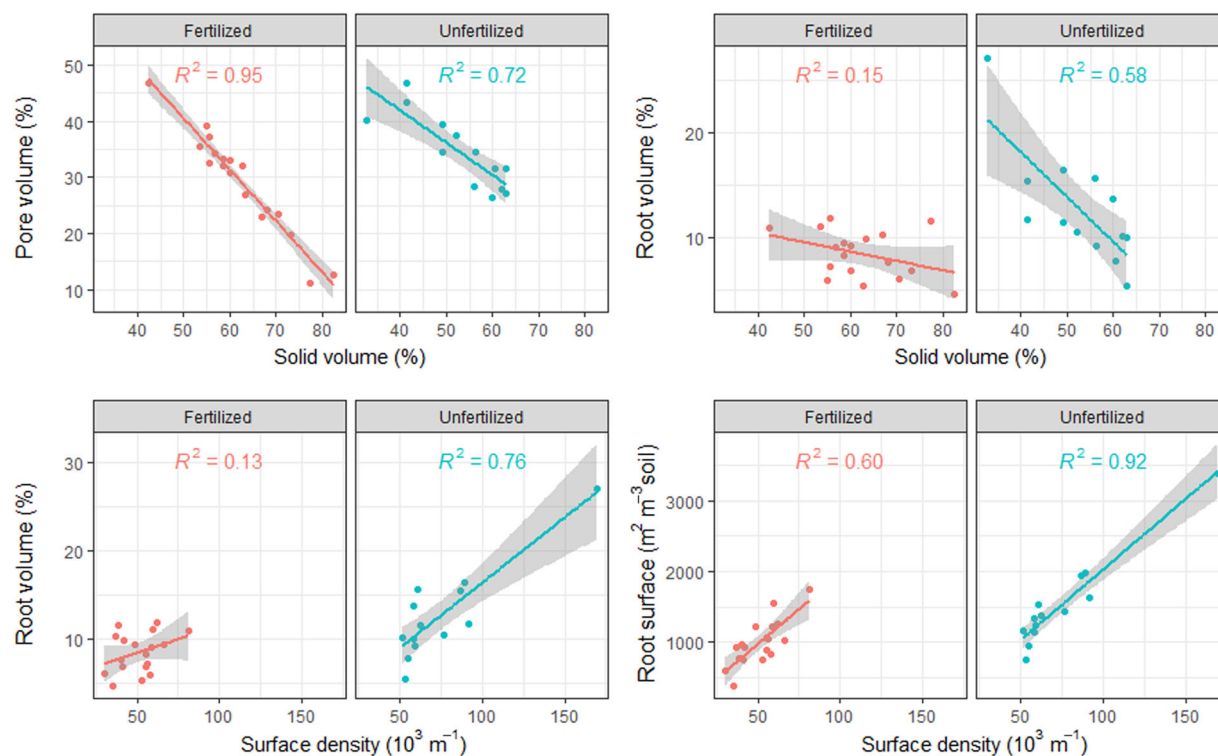


FIGURE 6 Relationship between soil structure and root development depending on fertilization as regression lines with 95% confidence intervals.

in SDen ($p < 0.01$) and SSurf ($p < 0.05$) and an increase of SV ($p < 0.05$) as Fe increases. According to the LM models, SDen and SSurf decrease by about 20% and 11%, respectively, and SV increases by 12% compared to the unfertilized plots when only $50 \text{ kg N ha}^{-1} \text{ year}^{-1}$ is applied. In contrast, PV appears to be most affected by M (Table 3), whereas the model explains only 13% ($p < 0.05$) of the variance of the dependent variable (Table 4). However, Figure 7 clearly shows that the PV decreases with increasing M. The second best model with PV as the dependent variable is also the model with Fe as the predictor variable (Table 3), so it can be assumed that fertilization also has an effect on PV. The LMs with the LUI parameters as predictor variables were not among the best candidate models, but since LUI is an integrating parameter for Fe, M, and G together, these models were also interpreted, as they all had a $\text{dAIC} > 2$ (Table S1). With the exception of PV LM, all models with LUI are also significant ($p < 0.05$) (Table S2). Figure S2 shows that SSurf, SDen, RV, and RSurf decrease with increasing LUI, while SV increases.

DISCUSSION

μCT is a very suitable method for simultaneous root and soil analysis in undisturbed soil cores (Helliwell et al., 2013; Mooney et al., 2012; Zhou et al., 2021). Figure 1 presents representative soil and root structures, combining two-dimensional μCT soil images with corresponding 3D μCT root images for a visual assessment of their spatial relationship. This visualization is crucial for comprehending belowground interactions, complementing the study's quantitative data. Figure S1 extends the

visual analysis with two additional replicates for each land use type, highlighting visual similarities. These consistent patterns support findings' validity and emphasize the importance of visual analysis. Initial observations hint at a potential link between soil structure and root patterns. The identification of root nodules in some samples adds intrigue, possibly indicating an active nitrogen-fixing process affecting nutrient availability (Mylona et al., 1995). These visual insights enhance our understanding of root–soil dynamics, adding a qualitative dimension to quantitative results. For instance, despite the potential exclusion of μCT -derived parameters as outliers in plot AEG25, both visual representations and quantitative data in Table 2 underscore its remarkably dense root network and well-structured soil. The data set consistently confirms these characteristics, demonstrating its reliability.

The measured μCT parameters (PV, SV, RV, SSurf, RSurf, and SDen) allow conclusions to be drawn for individual plots, for different land use types, for management differences such as M and Fe and for LUI with respect to root–soil characteristics. It seems that the different land use types and their land use intensity as meadow, mown pasture, or pasture play a crucial role in root development and soil structuring. The analysis of μCT parameters across different land use types revealed remarkable differences, especially in pastures, where root development and soil structure were significantly affected. It is also known that biodiversity is often higher on extensive pastures due to patch formation (Isselstein et al., 2005; Ludvíková et al., 2015), which could explain the significantly higher values for RV and RSurf. However, when focusing only on unfertilized plots, no significant differences were observed between meadows, mowed

TABLE 3 Ranking of best linear models with Akaike information criterion corrected for small sample size (AICc) differences of AICc (dAICc) for all μ CT parameters, that is, SV, RV, PV, SSurf, RSurf, and SDen.

Parameter	Linear models	AICc	dAICc
PV	$\lg(\text{PV}) \sim M$	-32.77	0.33
	$\lg(\text{PV}) \sim \sqrt{\text{Fe}}$	-31.36	0.16
	$\lg(\text{PV}) \sim \sqrt{G} + M$	-30.92	0.13
	$\lg(\text{PV}) \sim 1$	-30.69	0.12
SV	$\lg(\text{SV}) \sim \sqrt{\text{Fe}}$	-66.14	0.30
	$\lg(\text{SV}) \sim M$	-65.52	0.22
	$\lg(\text{SV}) \sim \sqrt{G} + M$	-64.30	0.12
	$\lg(\text{SV}) \sim 1$	-62.32	0.04
RV	$\lg(\text{RV}) \sim \sqrt{\text{Fe}}$	-28.43	0.43
	$\lg(\text{RV}) \sim \sqrt{G} + \sqrt{\text{Fe}}$	-26.31	0.15
	$\lg(\text{RV}) \sim M + \sqrt{\text{Fe}}$	-26.18	0.14
	$\lg(\text{RV}) \sim 1$	-21.12	0.01
SSurf	$\lg(\text{SSurf}) \sim \sqrt{\text{Fe}}$	-73.29	0.42
	$\lg(\text{SSurf}) \sim \text{LUI}$	-72.23	0.24
	$\lg(\text{SSurf}) \sim \text{LUI}_i + \text{LUI} + \text{LUI} : \text{LUI}_i$	-72.14	0.23
	$\lg(\text{SSurf}) \sim 1$	-68.68	0.04
RSurf	$\lg(\text{RSurf}) \sim \sqrt{\text{Fe}}$	-23.34	0.42
	$\lg(\text{RSurf}) \sim M + \sqrt{\text{Fe}}$	-21.17	0.14
	$\lg(\text{RSurf}) \sim \text{LUI}_i$	-20.85	0.32
	$\lg(\text{RSurf}) \sim 1$	-15.84	0.01
SDen	$\lg(\text{SDen}) \sim \sqrt{\text{Fe}}$	-33.65	0.41
	$\lg(\text{SDen}) \sim \text{LUI}$	-31.90	0.28
	$\lg(\text{SDen}) \sim \text{LUI}_i$	-31.80	0.27
	$\lg(\text{SDen}) \sim 1$	-28.14	0.03

Abbreviations: Fe, fertilization level; i, intercept; lg, logarithm to the base 10; LUI, Land Use Intensity Index; M, mowing frequency; PV, pore volume; RSurf, root surface; RV, root volume; SDen, surface density; SSurf, solid surface; SV, solid volume; μ CT, microcomputed tomography.

TABLE 4 Regression data of best LM for all μ CT parameters, that is, SV, RV, PV, SSurf, RSurf, and SDen.

LM	$\lg(\text{PV}) \sim M$	$\lg(\text{SV}) \sim \sqrt{\text{Fe}}$	$\lg(\text{RV}) \sim \sqrt{\text{Fe}}$	$\lg(\text{SSurf}) \sim \sqrt{\text{Fe}}$	$\lg(\text{RSurf}) \sim \sqrt{\text{Fe}}$	$\lg(\text{SDen}) \sim \sqrt{\text{Fe}}$
Intercept	1.542	1.721	1.066	3.550	3.146	1.831
Intercept SE	0.037	0.020	0.037	0.018	0.040	0.034
Slope	-0.048*	0.007*	-0.017**	-0.007*	-0.019**	-0.014**
Slope SE	0.023	0.002	0.005	0.003	0.005	0.004
R^2	0.13	0.18	0.27	0.20	0.27	0.23
F	4.58	6.51	10.74	7.43	10.98	8.50
p	0.041	0.016	0.003	0.011	0.003	0.007

Abbreviations: Fe, fertilization level; lg, logarithm to the base 10; LM, linear models; PV, pore volume; RSurf, root surface; RV, root volume; SDen, surface density; SE, standard error; SSurf, solid surface; SV, solid volume; μ CT, microcomputed tomography.

* $p < 0.05$, ** $p < 0.01$.

pastures and pastures. The limited sample size, especially the missing multiple unfertilized meadows, may contribute to the lack of statistical significance in this subset. By simply applying a straightforward approach of identifying

the maximum and minimum values of μ CT parameters, coupled with their corresponding plots, a discernible pattern was elucidated indicating the influence of land use intensity, as determined by the LUI, on both root

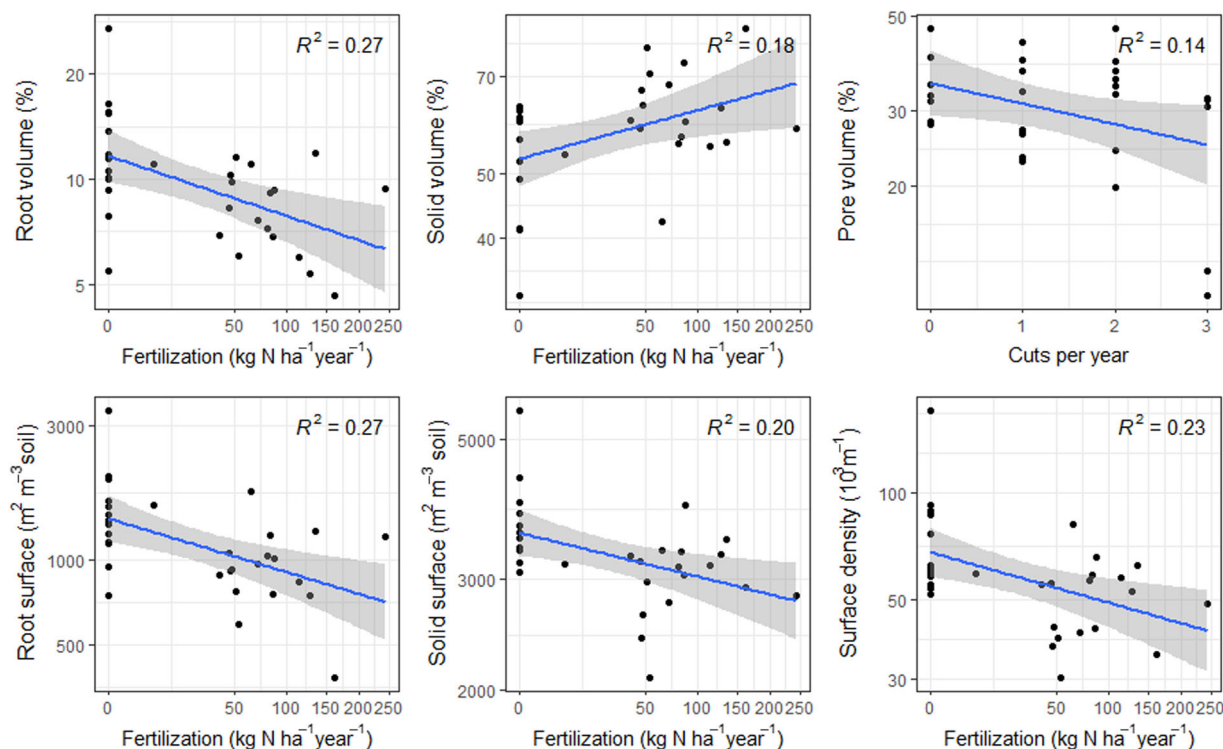


FIGURE 7 Relationship between dependent variables (all microcomputed tomography parameters) and its predictor variable from the best linear model (Table 3). Lines depict model predictions with 95% confidence intervals obtained from the best fitting.

growth and soil structuring. The comparative analysis between fertilized and unfertilized plots (Figure 3) reveals notable differences in μ CT parameters, except for PV. Unfertilized plots show a significant increase in root growth and an increased level of structural organization within the soil. This observation is supported by the application of LMs (Table 3), which indicate that Fe emerges as a central predictor for most parameters, explaining a considerable part of the variance. Increased Fe is associated with decreased RV and RSurf. The influence of Fe extends to soil structure, correlating with a decrease in SDen and SSurf and an increase in SV (Figure 7). These changes highlight the multifaceted effects of fertilization on both root and soil parameters. Similar results were found in a study by Holub et al. (2013), where increasing fertilization and especially N dosage generally led to better growth of aboveground plant parts, but not of underground roots. Contrasting studies have reported increased above- and belowground biomass in response to fertilization (Leuschner et al., 2013; Tomaškin et al., 2013). The specific factors contributing to this variation, such as experimental design, soil types or experiment duration, remain unclear and necessitate further investigation. It is crucial to note that our study exclusively focused on permanent grassland, which is commonly managed by farmers.

In our study, we also observed that as root development increased, the correlation between PV and SV decreased, while the relationship between root development and soil structure increased. Roots not only occupy PV but also actively contribute to soil lifting and loosening. Despite potential impediments such as soil compaction, our results suggest an

inverse relationship: improved soil structure is significantly associated with increased fine root development, particularly evident in a higher ratio of RSurf to RV.

The effects of fertilization on root development and soil structure in grasslands represent an important aspect of soil ecosystem dynamics with significant implications for ecosystem services (van Eekeren et al., 2010). The observed phenomenon that unfertilized grasslands show improved root development and soil structure compared to fertilized counterparts underscores the complex relationship between land management practices and soil health. Unfertilized grasslands show a notable advantage in root development. This phenomenon is likely due to the absence of external nutrient inputs, forcing plants to expand their root systems in search of essential nutrients (Hodge et al., 2009; Reynolds & D'Antonio, 1996). As a result, increased root biomass contributes to improved soil stability and structure (Angers & Caron, 1998; Bergmann et al., 2016). Increased root biomass leads to better soil aggregation (Graf & Frei, 2013), which facilitates better water infiltration and nutrient retention (Franzuebbers, 2002). In addition, the increased presence of roots stimulates microbial activity that promotes organic matter decomposition and nutrient cycling, thereby enhancing soil fertility (Cheng & Kuzyakov, 2005). The observed improvements in soil structure in unfertilized grasslands can be attributed to the interplay between root growth and soil stability. Exudates from roots act as binding agents, holding soil particles together and forming stable aggregates (Goss & Kay, 2005). This aggregation increases soil porosity, allowing for better air and water

movement, which is critical for nutrient availability and plant growth (Bronick & Lal, 2005). In addition, improved soil structure in unfertilized grasslands contributes to erosion control and reduces the risk of soil degradation. Conversely, fertilizer application alters this delicate balance by providing plants with external sources of nutrients. While this addition increases aboveground biomass and yield, it often comes at the expense of root development and soil structure (Holub et al., 2013). In fertilized grasslands, plants rely less on extensive root systems because readily available nutrients reduce the need for deep exploration. This can result in reduced root biomass and less developed root networks. In addition, overfertilization can lead to soil compaction and nutrient imbalances that negatively affect soil microbial communities and overall soil health. Mowing frequency also has an impact on soil compaction, as significantly higher SV was found for three cuts per year compared to pastures. However, three cuts per year is only an intermediate land use intensity that needs to be verified with higher numbers of cuts, since a trend but no significant differences could be found compared to one and two cuts per year. To study the impact of mowing frequency on soil and root parameters in more detail, further μ CT studies should be carried out on plots with up to six cuts per year on intensively managed plots. Our research findings notably support our third hypothesis, indicating that heightened land use intensity, marked by increased fertilization and mowing frequency, leads to diminished root growth and adverse effects on soil structure.

This study demonstrates the excellent suitability of μ CT for investigating the relationship between soil structure and root development, but also offers further potential for investigating soil as a habitat for soil organisms. These relationships make μ CT an objective and standardizable method to quantify soil quality and soil health. In addition, AI can play an important role in future work in the analysis of μ CT data, for which basic principles have already been developed (Wieland et al., 2021).

Future μ CT analyses will be conducted on other soil types to investigate the dependence of root development and soil structure on site-specific soil parameters such as clay and carbon content. In addition, μ CT will be used to study the soil as a habitat for soil organisms, for example, to elucidate relationships between microbiology or edaphon and soil structure and their influence on soil turnover processes and carbon sequestration.

CONCLUSIONS

The analysis of the μ CT parameters in relation to grassland management practices provides valuable insights into the soil and root characteristics. The comparison of data reveals distinct differences between various land uses and fertilizer applications, mowing frequency and in general depending of land use intensity. In summary, these findings suggest that grassland management practices, particularly fertilization and

mowing frequency, significantly influence soil structure and root development. Fertilization appears to notably affect root growth and soil structure, while mowing frequency correlates with soil structure changes. Understanding these relationships can aid in formulating more effective land management strategies tailored to specific soil and root characteristics. In conclusion, the contrasting effects of fertilization on root development and soil structure in grasslands illustrate a critical trade-off between immediate productivity gains and long-term soil health and ecosystem services. Unfertilized grasslands show superior root growth and enhanced soil structure, fostering a healthier soil ecosystem that supports various ecosystem services. Understanding these dynamics is essential for developing sustainable land management practices that prioritize soil health while optimizing agricultural productivity. This insight can guide policies and practices aimed at balancing productivity goals with the preservation and enhancement of soil ecosystem services and soil health.

AUTHOR CONTRIBUTIONS

Katrin Kuka: Conceptualization; data curation; formal analysis; investigation; methodology; validation; visualization; writing—original draft. **Monika Joschko:** Conceptualization; funding acquisition; project administration; supervision; writing—review and editing.

ACKNOWLEDGMENTS

We thank the managers of the three Exploratories, Kirsten Reichel-Jung, Swen Renner, Katrin Hartwich, Sonja Gockel, Kerstin Wiesner, and Martin Gorke, for their work in maintaining the plot and project infrastructure; Christiane Fischer and Simone Pfeiffer for giving support through the central office, Michael Owonibi for managing the central database, and Markus Fischer, Eduard Linsenmair, Dominik Hessenmöller, Jens Nieschulze, Daniel Prati, Ingo Schöning, François Buscot, Ernst-Detlef Schulze, Wolfgang W. Weisser, and the late Elisabeth Kalko for their role in setting up the Biodiversity Exploratories project. Fieldwork permits were issued by the responsible state environmental offices of Baden-Württemberg, Thüringen and Brandenburg (according to § 72 BbgNatSchG). We are grateful to the UGT team for their technical support in soil sampling. We thank Bernhard Illerhaus, BAM, for the μ CT analysis of the soil cores and the fruitful discussions. We would also like to thank Doreen Gabriel for helping us with the statistical analysis. This work was supported by Deutsche Forschungsgemeinschaft (DFG-Jo228/8-1).

CONFLICT OF INTEREST STATEMENT

The authors declare no conflicts of interest.

DATA AVAILABILITY STATEMENT

The data that support the findings of this study are openly available in the BEXIS database at <https://www.bexis.uni-jena.de/>, reference numbers ID31514, ID14686, ID14447, ID14446, ID16566, and ID16586.

ORCID

Katrin Kuka  <http://orcid.org/0000-0002-9867-725X>

REFERENCES

- Akaike, H. (1973). Maximum likelihood identification of Gaussian autoregressive moving average models. *Biometrika*, 60(2), 255–265. <https://doi.org/10.2307/2334537>
- Amelung, W., Tang, N., Siebers, N., Aehnelt, M., Eusterhues, K., Felde, V. J. M. N. L., Guggenberger, G., Kaiser, K., Kögel-Knabner, I., Klumpp, E., Knief, C., Kruse, J., Lehnndorff, E., Mikutta, R., Peth, S., Ray, N., Pechtel, A., Ritschel, T., Schweizer, S. A., ... Totsche, K. U. (2023). Architecture of soil microaggregates: Advanced methodologies to explore properties and functions. *Journal of Plant Nutrition and Soil Science*, 187(1), 17–50. <https://doi.org/10.1002/jpln.202300149>
- Angers, D. A., & Caron, J. (1998). Plant-induced changes in soil structure: Processes and feedbacks. *Biogeochemistry*, 42(1), 55–72. <https://doi.org/10.1023/A:1005944025343>
- Bergmann, J., Verbruggen, E., Heinze, J., Xiang, D., Chen, B., Joshi, J., & Rillig, M. C. (2016). The interplay between soil structure, roots, and microbiota as a determinant of plant–soil feedback. *Ecology and Evolution*, 6(21), 7633–7644. <https://doi.org/10.1002/ece3.2456>
- Blaser, S. R. G. A., Koebernick, N., Spott, O., Thiel, E., & Vetterlein, D. (2020). Dynamics of localised nitrogen supply and relevance for root growth of *Vicia faba* ('Fuego') and *Hordeum vulgare* ('Marthe') in soil. *Scientific Reports*, 10(1), 15776. <https://doi.org/10.1038/s41598-020-72140-1>
- Blüthgen, N., Dormann, C. F., Prati, D., Klaus, V. H., Kleinebecker, T., Hölzel, N., Alt, F., Boch, S., Gockel, S., Hemp, A., Müller, J., Nieschulze, J., Renner, S. C., Schöning, I., Schumacher, U., Socher, S. A., Wells, K., Birkhofer, K., Buscot, F., ... Weisser, W. W. (2012). A quantitative index of land-use intensity in grasslands: Integrating mowing, grazing and fertilization. *Basic and Applied Ecology*, 13(3), 207–220. <https://doi.org/10.1016/j.baae.2012.04.001>
- Bronick, C. J., & Lal, R. (2005). Soil structure and management: A review. *Geoderma*, 124(1–2), 3–22. <https://doi.org/10.1016/j.geoderma.2004.03.005>
- Calcagno, V. (2013). glmulti: Model selection and multimodel inference made easy. *R Package Version*, 1(7), 67.
- Carminati, A., Vetterlein, D., Weller, U., Vogel, H.-J., & Oswald, S. E. (2009). When roots lose contact all rights reserved. No part of this periodical may be reproduced or transmitted in any form or by any means, electronic or mechanical, including photocopying, recording, or any information storage and retrieval system, without permission in writing from the publisher. *Vadose Zone Journal*, 8(3), 805–809. <https://doi.org/10.2136/vzj2008.0147>
- Cheng, W., & Kuzakov, Y. (2005). Root effects on soil organic matter decomposition. *Roots and Soil Management: Interactions Between Roots and the Soil*, 48, 119–143. <https://doi.org/10.2134/agronmonogr48.c7>
- Chenu, C., & Stotzky, G. (2002). Interactions between microbes and soil particles: An overview. In P. M. Huang, J. Berthelin, J. M. Bollag, & N. Senesi (Eds.), *Interactions between soil particles and microorganisms: Impact on the terrestrial ecosystem*. Wiley.
- Doran, J. W., & Zeiss, M. R. (2000). Soil health and sustainability: Managing the biotic component of soil quality. *Applied Soil Ecology*, 15(1), 3–11. [https://doi.org/10.1016/S0929-1393\(00\)00067-6](https://doi.org/10.1016/S0929-1393(00)00067-6)
- van Eekeren, N., de Boer, H., Hanegraaf, M., Bokhorst, J., Nierop, D., Bloem, J., Schouten, T., de Goede, R., & Brussaard, L. (2010). Ecosystem services in grassland associated with biotic and abiotic soil parameters. *Soil Biology and Biochemistry*, 42(9), 1491–1504. <https://doi.org/10.1016/j.soilbio.2010.05.016>
- Fischer, M., Bosdorf, O., Gockel, S., Hänsel, F., Hemp, A., Hessenmöller, D., Korte, G., Nieschulze, J., Pfeiffer, S., Prati, D., Renner, S., Schöning, I., Schumacher, U., Wells, K., Buscot, F., Kalko, E. K. V., Linsenmair, K. E., Schulze, E. D., & Weisser, W. W. (2010). Implementing large-scale and long-term functional biodiversity research: The biodiversity exploratories. *Basic and Applied Ecology*, 11(6), 473–485. <https://doi.org/10.1016/j.baae.2010.07.009>
- Fox, J. (2003). Effect displays in R for generalised linear models. *Journal of Statistical Software*, 8, 1–27. <https://doi.org/10.18637/jss.v008.i15>
- Franzluubbers, A. J. (2002). Water infiltration and soil structure related to organic matter and its stratification with depth. *Soil and Tillage Research*, 66(2), 197–205. [https://doi.org/10.1016/S0167-1987\(02\)00027-2](https://doi.org/10.1016/S0167-1987(02)00027-2)
- Gilhaus, K., Boch, S., Fischer, M., Hölzel, N., Kleinebecker, T., Prati, D., Rupprecht, D., Schmitt, B., & Klaus, V. H. (2017). Grassland management in Germany: Effects on plant diversity and vegetation composition. *Tuexenia*, 37, 379–397. <https://doi.org/10.14471/2017.37.010>
- Goss, M. J., & Kay, B. D. (2005). Soil aggregation. *Roots and Soil Management: Interactions Between Roots and the Soil*, 48, 163–180.
- Graf, F., & Frei, M. (2013). Soil aggregate stability related to soil density, root length, and mycorrhiza using site-specific *Alnus incana* and *Melanogaster variegatus* s.l. *Ecological Engineering*, 57, 314–323. <https://doi.org/10.1016/j.ecoleng.2013.04.037>
- Hassink, J., Bouwman, L. A., Zwart, K. B., & Brussaard, L. (1993). Relationships between habitable pore space, soil biota and mineralization rates in grassland soils. *Soil Biology and Biochemistry*, 25(1), 47–55. [https://doi.org/10.1016/0038-0717\(93\)90240-C](https://doi.org/10.1016/0038-0717(93)90240-C)
- Heijs, A. W. J., de Lange, J., Schoute, J. F. T., & Bouma, J. (1995). Computed tomography as a tool for non-destructive analysis of flow patterns in macroporous clay soils. *Geoderma*, 64(3–4), 183–196. [https://doi.org/10.1016/0016-7061\(94\)00020-B](https://doi.org/10.1016/0016-7061(94)00020-B)
- Helliwell, J. R., Sturrock, C. J., Grayling, K. M., Tracy, S. R., Flavel, R. J., Young, I. M., Whalley, W. R., & Mooney, S. J. (2013). Applications of X-ray computed tomography for examining biophysical interactions and structural development in soil systems: A review. *European Journal of Soil Science*, 64(3), 279–297. <https://doi.org/10.1111/ejss.12028>
- Hodge, A., Berta, G., Doussan, C., Merchan, F., & Crespi, M. (2009). Plant root growth, architecture and function. *Plant and Soil*, 321(1), 153–187. <https://doi.org/10.1007/s11104-009-9929-9>
- Holub, P., Tůma, I., & Fiala, K. (2013). Effect of fertilization on root growth in the wet submontane meadow. *Plant, Soil and Environment*, 59(8), 342–347. <https://doi.org/10.17221/162/2013-PSE>
- Hou, L., Gao, W., der Bom, F., Weng, Z., Doolette, C. L., Maksimenko, A., Hausermann, D., Zheng, Y., Tang, C., Lombi, E., & Kopittke, P. M. (2022). Use of X-ray tomography for examining root architecture in soils. *Geoderma*, 405, 115405. <https://doi.org/10.1016/j.geoderma.2021.115405>
- Illerhaus, B., Jasiuniene, E., Goebbels, J., & Loethman, P. (2002). Investigation and image processing of cellular metals with highly resolving 3D microtomography (μCT). In *Proceedings SPIE 4503, developments in X-ray tomography III*, (7 January 2002); (pp. 201–204). <https://doi.org/10.1117/12.452846>
- Isselstein, J., Jeangros, B., & Pavlu, V. (2005). Agronomic aspects of biodiversity targeted management of temperate grasslands in Europe—A review. *Agronomy Research*, 3(2), 139–151.
- Juma, N. G. (1993). Interrelationships between soil structure/texture, soil biota/soil organic matter and crop production. *Geoderma*, 57(1–2), 3–30. [https://doi.org/10.1016/0016-7061\(93\)90145-B](https://doi.org/10.1016/0016-7061(93)90145-B)
- Kuka, K., Illerhaus, B., Fox, C. A., & Joschko, M. (2013). X-ray computed microtomography for the study of the root–soil relationship in grassland soils. *Vadose Zone Journal*, 12(4), 1–10. <https://doi.org/10.2136/vzj2013.01.0014>
- Kuka, K., Illerhaus, B., Fritsch, G., Joschko, M., Rogasik, H., Paschen, M., & Seyfarth, M. (2013). A new method for the extraction of undisturbed soil samples for X-ray computed tomography. *E-Journal of Nondestructive Testing*, 18(8), 1–8. <https://www.ndt.net/?id=14629>
- Leuschner, C., Gebel, S., & Rose, L. (2013). Root trait responses of six temperate grassland species to intensive mowing and NPK fertilisation: A field study in a temperate grassland. *Plant and Soil*, 373, 687–698. <https://doi.org/10.1007/s11104-013-1836-4>
- Ludvíková, V., Pavlů, V., Pavlů, L., Gaisler, J., & Hejčman, M. (2015). Sward-height patches under intensive and extensive grazing density in an *Agrostis capillaris* grassland. *Folia Geobotanica*, 50, 219–228. <https://doi.org/10.1007/s12224-015-9215-y>
- Mayel, S., Jarrah, M., & Kuka, K. (2021). How does grassland management affect physical and biochemical properties of temperate grassland soils? A review study. *Grass and Forage Science*, 76(2), 215–244. <https://doi.org/10.1111/gfs.12512>
- Mooney, S. J., Pridmore, T. P., Helliwell, J., & Bennett, M. J. (2012). Developing X-ray computed tomography to non-invasively image 3-D root systems architecture in soil. *Plant and Soil*, 352, 1–22. <https://doi.org/10.1007/s11104-011-1039-9>

- Mylona, P., Pawlowski, K., & Bisseling, T. (1995). Symbiotic nitrogen fixation. *The Plant Cell*, 7(7), 869–885. <https://doi.org/10.1105/tpc.7.7.869>
- Pagliai, M., & De Nobili, M. (1993). Relationships between soil porosity, root development and soil enzyme activity in cultivated soils. In L. Brussaard & M. J. Kooistra (Eds.), *Soil Structure/Soil Biota Interrelationships* (pp. 243–256). Elsevier. <https://doi.org/10.1016/B978-0-444-81490-6.50024-8>
- Perret, J. S., Al-Belushi, M. E., & Deadman, M. (2007). Non-destructive visualization and quantification of roots using computed tomography. *Soil Biology and Biochemistry*, 39(2), 391–399. <https://doi.org/10.1016/j.soilbio.2006.07.018>
- Pierret, A., Capowicz, Y., Moran, C. J., & Kretschmar, A. (1999). X-ray computed tomography to quantify tree rooting spatial distributions. *Geoderma*, 90(3–4), 307–326. [https://doi.org/10.1016/S0016-7061\(98\)00136-0](https://doi.org/10.1016/S0016-7061(98)00136-0)
- R Core Team. (2021). *R: A language and environment for statistical computing. Supplemental information references S* (Vol. 1, pp. 371–378). R Foundation for Statistical Computing.
- Reynolds, H. L., & D'Antonio, C. (1996). The ecological significance of plasticity in root weight ratio in response to nitrogen: Opinion. *Plant and Soil*, 185(1), 75–97. <https://doi.org/10.1007/BF02257566>
- Rillig, M. C., Wright, S. F., & Eviner, V. T. (2002). The role of arbuscular mycorrhizal fungi and glomalin in soil aggregation: Comparing effects of five plant species. *Plant and Soil*, 238(2), 325–333. <https://doi.org/10.1023/A:1014483303813>
- Russell, V. L. (2023). *emmeans: Estimated marginal means, aka least-squares means*. <https://CRAN.R-project.org/package=emmeans>
- Schmidt, S., Bengough, A. G., Gregory, P. J., Grinev, D. V., & Otten, W. (2012). Estimating root–soil contact from 3D X-ray microtomographs. *European Journal of Soil Science*, 63(6), 776–786. <https://doi.org/10.1111/j.1365-2389.2012.01487.x>
- Shi, X., Qin, T., Yan, D., Tian, F., & Wang, H. (2021). A meta-analysis on effects of root development on soil hydraulic properties. *Geoderma*, 403, 115363. <https://doi.org/10.1016/j.geoderma.2021.115363>
- Six, J., Elliott, E. T., & Paustian, K. (1999). Aggregate and soil organic matter dynamics under conventional and no-tillage systems. *Soil Science Society of America Journal*, 63(5), 1350–1358. <https://doi.org/10.2136/sssaj1999.6351350x>
- Strong, D. T., Wever, H. D., Merckx, R., & Recous, S. (2004). Spatial location of carbon decomposition in the soil pore system. *European Journal of Soil Science*, 55(4), 739–750. <https://doi.org/10.1111/j.1365-2389.2004.00639.x>
- Tang, Y., Horikoshi, M., & Li, W. (2016). ggfortify: Unified interface to visualize statistical results of popular R packages. *The R Journal*, 8(2), 474–485. <https://doi.org/10.32614/RJ-2016-060>
- Tomaškin, J., Jančovič, J., Vozár, L., & Tomaškinová, J. (2013). The effect of mineral fertilization on belowground plant biomass of grassland ecosystems. *Acta Universitatis Agriculturae et Silviculturae Mendelianae Brunensis*, 61(5), 1431–1440. <https://doi.org/10.11118/actaun201361051431>
- Tracy, S. R., Black, C. R., Roberts, J. A., McNeill, A., Davidson, R., Tester, M., Samec, M., Korošak, D., Sturrock, C., & Mooney, S. J. (2012). Quantifying the effect of soil compaction on three varieties of wheat (*Triticum aestivum* L.) using X-ray micro computed tomography (CT). *Plant and Soil*, 353(1–2), 195–208. <https://doi.org/10.1007/s11104-011-1022-5>
- Wickham, H., Chang, W., & Wickham, M. H. (2016). Package ‘ggplot2’. *Create Elegant Data Visualisations Using the Grammar of Graphics. Version*, 2(1), 1–189.
- Wieland, R., Ukawa, C., Joschko, M., Krolczyk, A., Fritsch, G., Hildebrandt, T. B., Schmidt, O., Filser, J., & Jimenez, J. J. (2021). Use of deep learning for structural analysis of computer tomography images of soil samples. *Royal Society Open Science*, 8(3), 201275. <https://doi.org/10.1098/rsos.201275>
- Zhang, H., He, H., Gao, Y., Mady, A., Filipović, V., Dyck, M., Lv, J., & Liu, Y. (2023). Applications of computed tomography (CT) in environmental soil and plant sciences. *Soil and Tillage Research*, 226, 105574. <https://doi.org/10.1016/j.still.2022.105574>
- Zhou, H., Whalley, W. R., Hawkesford, M. J., Ashton, R. W., Atkinson, B., Atkinson, J. A., Sturrock, C. J., Bennett, M. J., & Mooney, S. J. (2021). The interaction between wheat roots and soil pores in structured field soil. *Journal of Experimental Botany*, 72(2), 747–756. <https://doi.org/10.1093/jxb/eraa475>

SUPPORTING INFORMATION

Additional supporting information can be found online in the Supporting Information section at the end of this article.

How to cite this article: Kuka, K., & Joschko, M. (2024). Grassland management intensity determines root development, soil structure, and their interrelationship: Results of a regional study of Leptosols in the Swabian Alps. *Grassland Research*, 3(2), 171–186. <https://doi.org/10.1002/glr2.12077>